1   **25 September 2014 REVISION 2**

2   **Klebelsbergite, $Sb_4O_4SO_4(OH)_2$: stability relationships, formation in Nature, and**

3   **refinement of its structure**

4

5   Adam. J. Roper, Peter Leverett, Timothy D. Murphy, Peter. A. Williams*

6

7   *School of Science and Health, University of Western Sydney, Locked Bag 1797, Penrith, New*

8   *South Wales 2451, Australia*

9

10   and David E. Hibbs

11

12   *Faculty of Pharmacy, University of Sydney, Sydney, New South Wales 2006, Australia*

13

14   *E-mail: p.williams@uws.edu.au

15

16

17

18

19

20

21

22

23

24

25

26   **ABSTRACT**

27   The extent to which secondary Sb minerals control Sb dispersion in the supergene

28   environment is yet to be fully understood. Stability studies of klebelsbergite have been

29   undertaken to better understand its role in controlling Sb mobility and relationships with

30   other secondary Sb minerals. Solubility in aqueous 0.1084 M HNO$_3$ was determined at

31   298.15 K and the data obtained used to derive $\Delta G_f^\ominus$(klebelsbergite, s, 298.15 K) = –2056.4

32   ±5.0 kJ mol^{-1}. Solubility data have been used to deduce the conditions under which the

33   mineral can form as a thermodynamically stable phase. The single-crystal X-ray structure of

34   synthetic klebelsbergite has been determined 293 K and is essentially the same as that

35   reported earlier for atoms with Z ≥ 8. Crystal data: orthorhombic, space group $Pca2_1$, a =

36   5.7563(4), b = 11.2538(7), c = 14.8627(9) Å, V = 962.81(11) Å^3, Z = 4. Refinement

37   converged to R_1 = 0.0154 for 2206 unique reflections with $I > 2\sigma(I)$. The present study has

38   located the hydroxyl H atoms on both O5 and O9. The H-bond arrangements are somewhat

39   different to those proposed earlier with the quasi- linear O9-H…O3 interaction having

40   <(DHA) = 171(6)°. The O5 hydroxyl H atom lies in a different position to that proposed

41   earlier and is involved in a bifurcated H-bond arrangement with O2 and with itself in a

42   symmetry-related position, with <(DHA) = 133(5) and 125(5)°, respectively.

43

44   *Key words*: klebelsbergite, antimony, antimony sulfate, solubility, stability, structure,

45   hydrogen bonding

46

47

48

49   **Introduction**

50   Recent studies regarding the immobilisation of Sb in natural settings have drawn

51   attention to the fact that many potentially important Sb phases remain essentially unstudied

52   and associated geochemical processes are still quite poorly understood (Filella et al. 2009;

53   Leverett et al. 2012; Roper et al. 2012). Given that the secondary Sb minerals arise

54   overwhelmingly via the oxidation of sulfides and sulfosalts, it is surprising that very few of

55   them contain sulfate. This no doubt reflects both solubility properties and relationships with

56   other more stable phases. Known secondary Sb sulfate minerals are klebelsbergite,

57   $Sb_4O_4SO_4(OH)_2$, peretaite, $CaSb_4O_4(SO_4)_2(OH)_2 \cdot 2H_2O$ and coquandite, the most recently

58   discovered. Coquandite was originally assigned the formula $Sb_6O_8SO_4 \cdot H_2O$ on the basis of

59   chemical analyses (Sabelli et al. 1992), but pervasive twinning in the crystals examined made

60   a complete structural characterisation impossible. The structure now has been determined by

61   single-crystal X-ray methods (Bindi et al. in review) and the formula is more correctly

62   $Sb_{6+x}O_{8+x}(SO_4)(OH)_x \cdot (H_2O)_{1-x}$ (x = 0.3 in the material examined). Of these only

63   klebelsbergite is known synthetically (Mercier et al. 1975, 1976; Menchetti and Sabelli

64   1980a; Nakai and Appleman 1980). We note that several other salts in the system Sb_2O_3-SO_3-

65   H_2O are known synthetically, including $Sb_2O_4SO_4$, $Sb_2O_2SO_4$, $Sb_2O(SO_4)_2$, $Sb_4O_3(SO_4)_3$,

66   $Sb_4O_5SO_4$, $Sb_6O_7(SO_4)_2$ and $SbOHSO_4 \cdot H_2O$ (Mercier et al. 1975; Bovin 1976; Douglade et

67   al. 1978; Gospodinov and Ojkova 2004; Bergmann and Koparal 2007); none of these has

68   been shown to exist in Nature.

69   The three sulfate minerals reported to date have a remarkably similar association and

70   paragenesis. Coquandite is known from three localities in Tuscany, Italy, the Ribeiro da Serra

71   mine, Gondomar, Portugal, and the Lucky Knock mine, Tonasket, Washington, USA. In the

3

72   Pereta mine, Tuscany, it always occurs with klebelsbergite and peretaite, in association with

73   valentinite, Sb_2O_3, sénarmontite, Sb_2O_3, stibiconite, *ca* $SbSb_2O_6(OH)$, gypsum, $CaSO_4·2H_2O$,

74   and native sulfur (Cipriani et al. 1980a). It is an acid alteration product of stibnite, as is the

75   case in the La Cetine mine, Tuscany, from which peretaite and klebelsbergite are also known

76   (Sarp et al. 1983; Sabelli et al. 1992). At the Lucky Knock mine, fibres and plates of

77   coquandite are associated with stibnite and stibiconite (Sabelli et al. 1992). The coquandite-

78   klebelsbergite-peretaite assemblage is also found in the third Tuscan deposit, the Micciano

79   mine, associated with cervantite, Sb_2O_4, stibiconite and native sulfur (Orlandi 1984, 1997).

80   Klebelsbergite, cervantite, valentinite and sénarmontite occur in association at the Ribeiro da

81   Serra mine as oxidation products of stibnite and metastibnite, Sb_2S_3. Attention is drawn to the

82   native sulfur association, characteristic of rapid oxidation of sulfide under acidic conditions

83   (Williams 1990). Peretaite (Cipriani et al. 1980b; Menchetti and Sabelli 1980b) is known

84   only from the three Tuscan localities mentioned above.

85   Klebelsbergite is the most common secondary sulfate and has been reported from

86   eight localities; its associations in several of them have been outlined immediately above. In

87   the Chauvai Sb-Hg deposit, Kyrgyzstan, Russia, it occurs as an oxidation product of stibnite

88   together with cervantite, sénarmontite, stibiconite and valentinite (Kolesar et al. 1993). Little

89   information is available on its occurrence at the type locality, Baia Sprie, Romania, other than

90   it is an alteration product of stibnite (Palache et al. 1951). The single-crystal structure of

91   klebelsbergite was determined originally by Menchetti and Sabelli (1980a).

92   Here we report a study of the stability of klebelsbergite at 298.15 K and the conditions

93   under which it may form in oxidised Sb deposits. In addition we have re-determined the

94   single-crystal X-ray structure of the mineral. Details concerning the hydrogen bonding

95   network have been resolved.

96

4

97   **Experimental**

98   *Synthesis*

99   Following the synthesis of Nakai and Appleman (1980), Sb_2O_3 (2.0g, 6.861 mmol)

100   was heated under reflux in 600 cm^3 of aqueous 0.56 M H_2SO_4 for 6 days. The resulting solid,

101   obtained in essentially quantitative yield, consisted of transparent crystals with apparent

102   twinning up to 0.3 mm in size. Powder X-ray diffraction studies of the product (Philips

103   PW1825/20 powder diffractometer, Ni-filtered Cu$K\alpha_1$ radiation, $\lambda = 1.5406$ Å, 40 kV, 30

104   mA) showed the presence only of klebelsbergite. Unit cell parameters refined from the

105   powder X-ray data using LAPOD (Langford, 1973) are $a = 5.7563(4)$, $b = 11.2538(7)$, $c =$

106   14.8627(9) Å. These compare favourably with those of Menchetti and Sabelli (1980a), $a =$

107   5.776(2), $b = 11.274(2)$, $c = 14.887(2)$ Å, and Nakai and Appleman (1980), $a = 5.7648(6)$, b

108    $= 11.279(2)$, $c = 14.909(3)$ Å.

109   *X-ray single-crystal structure*

110   Single-crystal X-ray diffraction data were collected using a Bruker APEX2 CCD

111   diffractometer at 293(2) K with graphite-monochromated Mo$K\alpha$ radiation ($\lambda = 0.71073$ Å)

112   and corrected for Lorentz and polarization effects. An empirical absorption correction was

113   made based on psi-scans.

114   *Solubility studies*

115   Solubility studies were undertaken using sealed 250 cm^3 conical Quickfit[R] flasks in a

116   25.0 ±0.2°C thermostatted water bath. Measurements of pH were made using a Radiometer

117   ION450 apparatus fitted with a combination electrode.

118   To determine the solubility of klebelsbergite, finely ground solid (*ca* 0.1 g) was added

119   to each flask (n = 6), together with 100 cm^3 of standardised 0.1084 M HNO_3. The flasks were

120   left for 14 weeks with occasional stirring, while a paired flask was monitored periodically for

121   pH until no change was detected. Equilibrium was achieved after 2 weeks. Equilibrated

5

122   solutions were filtered off using Whatman^R GF/F fibreglass filters and collected in clean PET

123   bottles. Powder XRD measurements of the recovered solids showed no evidence that the

124   mineral dissolves congruently. Dissolved Sb concentrations determined using ICP-MS with

125   matched standards are listed in Table 1 and these define the solubility of the mineral.
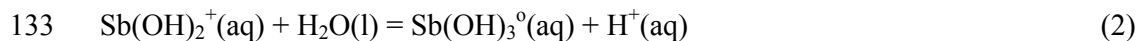
126

127   **Results and discussion**

128   *Solubility and stability studies*

129   The dissolution can be expressed by equation (1). Total dissolved Sb concentrations

130   in 0.1084 *M* HNO at 298.15 K are listed in Table 1.

131

132   $Sb_4O_4SO_4(OH)_2(s) + 6H_2O(l) = 4Sb(OH)_3^o(aq) + SO_4^{2-}(aq) + 2H^+(aq)$ (1)

133   $Sb(OH)_2^+(aq) + H_2O(l) = Sb(OH)_3^o(aq) + H^+(aq)$ (2)

134   $SO_4^{2-}(aq) + H^+(aq) = HSO_4^-(aq)$ (3)

135

136   The pH at equilibrium (1.055) was used in the determination of solution speciation

137   (hydrolysed Sb(III) species and HSO_4^-) using COMICS (Perrin and Sayce 1969). Stability

138   constants for equations (2) and (3) at 298.15 K were taken from Baes and Mesmer (1976) and

139   corrected for ionic strength ($I = 0.108$). Appropriate species concentrations at equilibrium

140   were converted to activities using the Davis extension of the Debye-Hückel equation [lg γ = −

141   $0.5085z^2(\sqrt{I}/(1+\sqrt{I}) − 0.3I)$; γ = activity coefficient, z = charge, I = ionic strength], with γ^o

142   (activity coefficient for neutral species) set at 1. The activity of H^+(aq) was from the direct

143   measurement of the pH at equilibrium. The derived activities yield a value of lg K for

144   equation (1) of −25.57 ±0.10. Use of the appropriate data in Table 2 for equation give

145   $\Delta G_f^e(Sb_4O_4SO_4(OH)_2, s, 298.15 K) = −2056.4 ±5.0$ kJ mol^{-1}. The estimated error takes into

146   account the analytical error of the solubility experiments, errors quoted for the

6

147   thermochemical data used, and an estimated error of ± 1.0 kJ mol^{-1} for $\Delta G_f^\ominus$(Sb(OH)$_3^o$, aq,

148   298.15 K).

149   A Pourbaix diagram illustrating stability relations between klebelsbergite with respect

150   to some common secondary Sb minerals and stibnite is shown in Figure 1. Thermochemical

151   data used to construct it are listed in Table 2. Klebelsbergite occupies a field between

152   kermesite and cervantite which increases with increasing $a(\text{SO}_4^{2-})$, as expected, and is stable

153   with respect to Sb$_2$O$_3$, valentinite and sénarmontite, under acidic conditions. The common

154   association of these minerals in Nature is thus seen to reflect a subtle pH variation in

155   mineralising solutions. Nevertheless, it must be emphasised that the indicated stability field

156   for klebelsbergite in Figure 1 could be misleading in another sense. It takes no account of the

157   possible influence of other dissolved species, cations in particular, and these will undoubtedly

158   serve to give rise to different phases (Leverett et al. 2012; Roper et al. 2012). Natural

159   mineralising solutions are anything but as simple as those stipulated by the conditions

160   considered above. For example, the relationship of klebelsbergite and schafarzikite is

161   described by equation (4).

162

163   Sb$_4$O$_4$SO$_4$(OH)$_2$(s) + 2Fe^{2+}(aq) + 2H$_2$O(l) = 2FeSb$_2$O$_4$(s) + SO$_4^{2-}$ (aq) + 6H$^+$(aq)   (4)
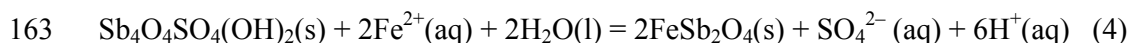
164

165   Using values reported in Table 2, $\Delta G_r^\ominus$(298.15 K) = +47.8 kJ mol^{-1} corresponding to

166   lg K = –8.37. With $a(\text{SO}_4^{2-})$ = 10^{-2}, $a(\text{Fe}^{2+})$ = –6 and –2 renders klebelsbergite unstable above

167   pH 3.06 and 1.73, respectively. As $a(\text{Fe}^{2+})$ increases and/or $a(\text{SO}_4^{2-})$ decreases, the stability

168   field for klebelsbergite is minimised, with klebelsbergite only stable under acidic conditions

169   with respect to schafarzikite. Under highly oxidising conditions, klebelsbergite reacts to form

170   more stable Sb(V) minerals, such as cervantite shown in Figure 1. In the presence of minor

171   Fe^{3+}, cervantite is unstable with respect to tripuhyite, as is klebelsbergite. The impact of

7

172   roméite group minerals is also an important consideration for the stability field of

173   klebelsbergite and investigations are underway in our laboratory to determine reliable

174   thermochemical data for these phases. Taking all of these matters into account, the rarity of

175   klebelsbergite is understandable. Relations with coquandite remain unknown and peretaite

176   may form preferentially, metastably or otherwise, in the presence of Ca^{2+} ions. Taking the

177   above into account, klebelsbergite will not exert a particularly significant influence in

178   controlling Sb dispersion in the natural environment except in particular circumstances, as

179   outlined above.

180   *X-ray single-crystal structure*

181   Details concerning data collection and refinement are given in Table 3. Final atom

182   coordinates and equivalent isotropic displacement parameters are listed in Table 4 and

183   anisotropic displacement parameters in Table 5. Selected bond lengths and angles are given

184   in Table 6. Statistical analysis of the data clearly indicated that the structure adopted the non-

185   centrosymmetric space group *Pca2$_1$* and the structure was solved by direct methods using

186   SHELXS-97 (Sheldrick 2008). The expected four antimony, single sulfur and ten oxygen

187   atom positions were readily located, and found to be in good agreement with those originally

188   reported by Menchetti and Sabelli (1980a). A least-squares refinement using SHELXL-97

189   converged smoothly with isotropic displacement parameters for all atoms to a $R_1 = 0.023$.

190   The refinement indicated significant twinning to be present and in a subsequent anisotropic

191   refinement a simple twin law with (001) as the twin plane, as predicted by Menchetti and

192   Sabelli (1980a), was invoked, resulting in twin components of 0.43:0.57 and $R_1 = 0.016$. A

193   difference Fourier then revealed the positions of the two expected hydroxyl H atoms on O5

194   and O9. In a final refinement the H atom positions were refined with soft restraints using a

195   riding model and with isotropic thermal parameters, resulting in a final R_1 and wR_2 of 0.0154

196   and 0.0377, respectively, for 2201 reflections with $I > 4\sigma(I)$. The weighting scheme used was

197     $w = 1/[\sigma^2(Fo^2) + (0.0166P)^2 + 1.46P]$, where $P = [\max(0, F_o)^2 + (2F_c)^2]/3$, as defined by

198   SHELXL.

199   The structure of klebelsbergite originally reported by Menchetti and Sabelli (1980a)

200   has been confirmed in this study, where the superior X-ray data set has now allowed some

201   structural aspects mentioned by the above authors to be clarified. The structure is most

202   simply described as edge-sharing of Sb^{3+}-O polyhedra forming layers parallel to (001), with

203   adjacent layers linked directly via shared oxygen atoms of SO_4^{2-} tetrahedra and indirectly via

204   H-bonds associated with OH groups coordinated to two of the four crystallographically

205   independent Sb^{3+} ions (Figure 2).

206   The four independent Sb^{3+} ions are bonded to four O atoms with bond lengths ranging

207   from 1.949 to 2.518 Å. In each case the O atoms are located to the side of the central Sb^{3+} ion

208   so that it lies effectively out of the centre of its coordination polyhedron. This is common for

209   ions such as Sb^{3+} which are considered to have one unshared electron pair (*E*), where the

210   theoretical centre of this lone pair has been calculated to lie ~1.1 Å from the Sb^{3+} ion (Galy *et*

211   *al*., 1975). In klebelsbergite the coordination of each of the four Sb^{3+} ions is similar (Table 6)

212   and may be described as distorted SbO_4E trigonal bipyramidal, where in each case there are

213   two equatorial Sb-O bonds of ~2.0 Å and two slightly longer axial Sb-O bonds of ~2.1 to

214   ~2.3 Å; Sb3 possesses one somewhat longer axial Sb-O distance at ~2.5 Å. The angles

215   between the two equatorial Sb-O bonds are ~91° for all but one of the Sb^{3+} polyhedra (Sb2),

216   which has an angle of ~98$^°$, while the dihedral angles between the two axial Sb-O bonds

217   range from ~140-150°. These values may be compared with the theoretical values of 92.2 and

218   151.5° proposed by Galy et al. (1975). A more detailed discussion of the Sb coordination is

219   given in the original crystal structure determination by Menchetti and Sabelli (1980a). In this

220   original work the hydroxyl oxygen atoms were correctly identified as O5 and O9, and both

221   are bonded to only one Sb atom. However, the associated H atoms could not be located. They

9

222   were hence positioned on the basis of crystal-chemical considerations, assuming an O-H

223   bond length of ~1.0 Å and a linear H-bond from the donor atoms O5 and O9 to the probable

224   sulfate oxygen acceptors, O2 and O3 respectively (these being at a contact distance of ~2.9 Å

225   and not linked to an Sb atom). The present study has located the hydroxyl H atoms on both

226   O5 and O9, and confirms the proposed H-bond arrangement for O9-H…O3 of Menchetti and

227   Sabelli (1980a) although the bond is not quite linear (Table 6). However, the O5 hydroxyl H

228   atom lies in a different position to that proposed by Menchetti and Sabelli (1980a) and does

229   not form a simple linear O5-H…O2 link. It is involved in a bifurcated H-bond system with

230   O2 and O5' in a symmetry-related position (Table 6). The hydrogen bonding scheme is

231   illustrated in Figure 3. As a consequence of the different roles played by the oxygen atoms of

232   the SO_4^{2-} tetrahedra in the linkage of the Sb-O sheets, where O1 and O4 are also bonded to an

233   Sb^{3+} ion while O2 and O3 are just weak H-bond acceptors, Menchetti and Sabelli (1980a)

234   pointed out that this should be reflected in the S–O1 and S–O4 distances being longer than

235   those for S–O2 and S–O3. This was not evident in their results, but it is nicely demonstrated

236   in the current structural study (Table 6). Nakai and Appleman (1980) reported a single O–H

237   stretch in the IR of klebelsbergite at 3435 cm^{-3}. Subsequently, Frost and Bahfenne (2010)

238   reported the Raman spectrum of the mineral. The band centred at ~3435 cm^{-3} could be

239   deconvoluted to give a sharper component at 3435 cm^{-3} and a weaker, broad component at

240   3457 cm^{-3}. The former may be attributed to the *quasi*-linear O(9)-H(2)...O(3) H-bond and the

241   latter to the bifurcated one. A third, still weaker and broad component at 3357 cm^{-3} may be

242   attributed to adsorbed water.

243   Finally, in their discussion of the klebelsbergite structure Menchetti and Sabelli

244   (1980a) noted the marked pseudo-centrosymmetric nature of the Sb-O layers, which lie

245   parallel to (001), and concluded that the presence of this pseudosymmetry could well lead to

246   twinning with (001) being the twin plane. In the present study, while it has been shown

247   conclusively that the structure of klebelsbergite is non-centrosymmetric, space group $Pna2_1$,

248   it was noted that the E-value statistics for the $hk0$ reflections strongly suggested a

249   centrosymmetric aspect to the structure which of course is in line with a pseudo-inversion

250   centre present in the Sb-O sheets. In line with the suggestion, the crystal used here for the

251   single-crystal structure determination was found to be significantly twinned, with twin

252   components of 0.43 and 0.57 and the twin plane is (001), as suggested by Menchetti and

253   Sabelli (1980a).

254

255   **Implications**

256   The structure of klebelsbergite reported here represents a refinement of that reported

257   earlier by Menchetti and Sabelli (1980a) and confirms some of the details of geometry that

258   had been incompletely proven. In particular, accurate location of the H atoms has established

259   the true nature of the hydrogen bonding scheme. Measurement of the solubility of the mineral

260   in aqueous H_2SO_4 gives $\Delta G_f^{\ominus}(Sb_4O_4SO_4(OH)_2, s, 298.15 K) = -2056.4 \pm 5.0$ kJ mol^{-1}. This

261   quantity has been used to evaluate the conditions under which the mineral forms as a

262   thermodynamically stable phase in Nature. Sulfate is of course a most important ion in the

263   vicinity of oxidizing sulfides, the geochemical environment in which klebelsbergite is found.

264   It is quite surprising, given the fact that high sulfate activities will be associated with

265   oxidizing Sb ores, that the stability field for the mineral under ambient conditions is

266   somewhat restricted. Nevertheless, this study unambiguously establishes the conditions

267   necessary for the formation of the mineral and this is of importance in light of current

268   research on the environmental geochemistry of Sb. Such information is of particular

269   significance for studies concerning Sb pollution, because of the metal's toxicity. In the light

270   of the above, klebelbergite will not be a useful sink for immobilising Sb.

271

272   **Supplementary material**

273   Full lists of crystallographic data excluding structure factor tables have been

274   deposited with the Inorganic Crystal Structure Database (ICSD), Fachinformationszentrum,

275   Karlsruhe, Germany; CRYSDATA@FIZ-Karlsruhe.DE. Any request to the ICSD for this

276   material should quote the full literature citation and the CSD-number 427364 (filename H2

277   O10 S Sb4). Lists of observed and calculated structure factors are available from the authors

278   upon request.

279

280   **References**

281   Babčan, J. (1976) Enstehung und Stabilität von Antimonmineralen im System Sb^{3+} - S^{2-} - H^+-

282   OH^-. Chemie der Erde, 35, 281-284 (in German).

283   Baes, C.F. Jr., and Mesmer, R.E. (1976) The Hydrolysis of Cations, 490 p. Wiley

284   Interscience, New York.

285   Bergmann, M.E.H., and Koparal, A.S. (2007) Kinetic studies on electrochemical antimony

286   removal from concentrated sulfuric acid systems. Chemical Engineering and Technology,

287   30, 242-249.

288   Bovin, J.-O. (1976) The crystal structure of the antimony(III) oxide sulfate $Sb_6O_7(SO_4)_2$. Acta

289   Crystallographica, B32, 177l-1777.

290   Bryndzia, L.T., and Kleppa, O.J. (1988) High temperature reaction calorimetry of solid and

291   liquid phases in part of the quasi-binary system Cu_2S-Sb_2S_3. American Mineralogist, 73,

292   707-713.

293   Cipriani, N., Menchetti, S., and Sabelli, C. (1980a) Klebelsbergite and another antimony

294   mineral from Pereta, Tuscany, Italy. Neues Jahrbuch für Mineralogie, Monatshefte, 223-

295   229.

296   Cipriani, N., Menchetti, S., Orlandi, P., and Sabelli, C. (1980b) Peretaite,

297         $CaSb_4O_4(OH)_2 \cdot 2H_2O$, a new mineral from Pereta, Tuscany, Italy. American

298   Mineralogist, 65, 936-939.

299   Cox, J.D., Wagman, D.D., and Medvedev, V.A. (1989) CODATA Key Values for

300   Thermodynamics, 271 p. Hemisphere Press, New York.

301   Douglade, J., Mercier, R., and Vivier, H. (1978) Structure crystalline de

302         $Sb_2(OH)_2(SO_4)_2 \cdot 2H_2O$. Acta Crystallographica, B34, 3163-3168 (in French).

303   Filella, M., Williams, P.A., and Belzile, N. (2009) Antimony in the environment: knowns and

304   unknowns. Environmental Chemistry, 6, 95-105.

305   Frost, R.L., and Bahfenne, S. (2010) A Raman spectroscopic study of the antimony mineral

306   klebelsbergite $Sb_4O_4(OH)_2(SO_4)$. Journal of Raman Spectroscopy, 42, 219-223.

307   Galy, J., Meunier, G., Andersson, S., and Åström, A. (1975) Stéréochimie des eléments

308   comportant des paires non liées: Ge (II), As (III), Se (IV), Br (V), Sn (II), Sb (III), Te

309   (IV), I (V), Xe (VI), Tl (I), Pb (II), et Bi (III) (oxydes, fluorures et oxyfluorures). Journal

310   of Solid State Chemistry, 13, 142-159 (in French).

311   Gospodinov, G., and Ojkova, D.T. (2004) Untersuchung der Phasengleichgewichte in den

312   Systemen Sb_2O_3-SO_3-H_2O und Bi_2O_3-SO_3-H_2O. Zeitschrift für anorganische und

313   allgemeine Chemie, 472, 233-240 (in German).

314   Kolesar, P., Brekler, V., and Tvrdý, J. (1993) Südkirgisien, Quecksilber-Antimon-

315   Lagerstätten und ihre Mineralien. Lapis, 18, 11-24 (in German).

316   Langford, J.I. (1973) Least-squares refinement of cell dimensions from powder data by

317   Cohen's method. Journal of Applied Crystallography, 6, 190-196.

318   Leverett, P., Reynolds, J.K., Roper, A.J., and Williams, P.A. (2012) Tripuhyite and

319   schafarzikite: two of the ultimate sinks for antimony in the natural environment.

320   Mineralogical Magazine, 76, 891-902.

321   Menchetti, S., and Sabelli, C. (1980a) The crystal structure of klebelsbergite,

322          $Sb_4O_4(OH)_2SO_4$. American Mineralogist, 65, 931-935.

323   Menchetti, S., and Sabelli, C. (1980b) Peretaite, $CaSb_4O_4(OH)_2(SO_4)_2 \cdot 2H_2O$: its atomic

324   arrangement and twinning. The crystal structure of klebelsbergite, $Sb_4O_4(OH)_2SO_4$.

325   American Mineralogist, 65, 940-946.

326   Mercier, R., Douglade, J., and Theobald, F. (1975) Structure crystalline de $Sb_2O_3 \cdot 2SO_3$. Acta

327   Crystallographica, B31, 2081-2085 (in French).

328   Mercier, R., Douglade, J., and Bernard, J. (1976) Structure crystalline de $Sb_2O_3 \cdot 3SO_3$. Acta

329   Crystallographica, B32, 2787-2791 (in French).

330   Nakai, I., and Appleman, D.E. (1980) Klebelsbergite, $Sb_4O_4(OH)_2SO_4$: redefinition and

331   synthesis. American Mineralogist, 65, 499-505.

332   Orlandi, P. (1984) Segnalazione di nuove specie mineralogiche in località italiane [peretaite,

333   klebelsbergite a Micciano - PI]. Rivista Mineralogica Italiana, 8, 33-40 (in Italian).

334   Orlandi, P. (1997) Zibaldone di mineralogia italiana [brabantite e torite di Botro ai Marmi;

335   coquandite di Micciano; kutnohorite del temperino; mimetite, cerussite ed emimorfite del

336   Monte Tambura]. Rivista Mineralogica Italiana, 21, 179-185 (in Italian).

337   Palache, C., Berman, H., and Frondel, C. (1951) The System of Mineralogy. John Wiley and

338   Sons, New York, Volume II, p. 583.

339   Pankajavalli, R., and Sreedharan, O.M. (1987) Thermodynamic stability of Sb_2O_4 by a solid

340   oxide electrolyte e.m.f. method. Journal of Materials Science, 22, 177-180.

341   Perrin, D.D., and Sayce, I.G. (1967) Computer calculation of equilibrium concentrations in

342   mixtures of metal ions and complexing species. Talanta, 14, 833-842.

343   Robie, R.A., and Hemingway, B.S. (1995) Thermodynamic properties of minerals and related

344   substances at 298.15 K and 1 bar (10^5 Pascals) pressure and at higher temperatures.

345   *United States Geological Survey Bulletin*, 2131.

346   Roper, A.J., Williams, P.A., and Fillela, M. (2012) Secondary antimony minerals: phases that

347   control the dispersion of antimony in the supergene zone. Chemie der Erde, 72S4, 9-14.

348   Sabelli, C., Orlandi, P., and Vezzalini, G. (1992) Coquandite, $Sb_6O_8(SO_4).H_2O$, a new

349   mineral from Pereta, Tuscany, Italy, and two other localities. Mineralogical Magazine,

350   56, 599-603.

351   Sarp, H., Perroud, P., and Deferne (1983) Présence de peretaite, $CaSb_4O_4(OH)_2(SO_4)_2 \cdot 2H_2O$,

352   dans la mine de Cetine (Toscane, Italie). Archives des Sciences, Genève, 36, 345-347 (in

353   French).

354   Seal, R.R., II, Robie, R.A., Hemingway, B.S., and Barton, P.B. Jr. (1992) Superambient heat

355   capacities of synthetic stibnite, berthierite and chalcostibite: revised thermodynamic

356   properties and implications for phase equilibria. Economic Geology, 87, 1911-1918.

357   Sheldrick, G.M. (2008) A short history of SHELX. Acta Crystallographica, A64, 112-122.

358   Williams, P.A. (1990) Oxide zone geochemistry, 286 p. Ellis Horwood, Chichester.

359   Williams-Jones, A.E., and Normand, C. (1997) Controls on mineral parageneses in the

360   system Fe-Sb-S-O. Economic Geology, 92, 308-324.

361   Zotov, A.V., Shikina, N.D., and Akinfiev, N.N. (2003) Thermodynamic properties of the

362   Sb(III) hydroxide complex $Sb(OH)_3(aq)$ at hydrothermal conditions. Geochimica et

363   Cosmochimica Acta, 67, 1821-1836.

364

365

366 Table 1. Dissolved Sb concentrations for the klebelsbergite equilibrations at 298.15 K.

	10^5[Sb]/mol dm^{-3}	pH
1	7.802	1.054
2	7.966	1.052
3	7.638	1.053
4	8.213	1.059
5	8.213	1.056
6	7.556	1.052
Mean	7.901	1.055
Error	±0.329	±0.004

367
368
369
370
371
372

373 Table 2. Thermodynamic quantities used in the calculations (T = 298.15 K).

		$\Delta G_f^{\ominus}$/kJ mol^{-1}	References
Stibnite	$Sb_2S_3(s)$	−149.9±2.1	Bryndzia and Kleppa (1988); Seal et al. (1992)
Kermesite	$Sb_2S_2O(s)$	−406.5	Williams-Jones and Normand (1997); Babčan (1976)
Sénarmontite	$Sb_2O_3(s)$	−633.2±2.1	Zotov et al. (2003)
Valentinite	$Sb_2O_3(s)$	−625.9±2.1	Zotov et al. (2003)
Cervantite	$Sb_2O_4(s)$	−754.5±1.6	Pankajavalli and Sreedharan (1987)
Tripuhyite	$FeSbO_4(s)$	−836.8 ±2.2	Leverett et al. (2012)
Schafarzikite	$FeSb_2O_4(s)$	−959.4±4.3	Leverett et al. (2012)
Klebelsbergite	$Sb_4O_4SO_4(OH)_2(s)$	−2056.4±5.0	this study
	$SO_4^{2-}(aq)$	−744.0±0.4	Cox et al. (1989)
	$H_2O(l)$	−237.1±0.1	Cox et al. (1989)
	$Fe^{2+}(aq)$	−90.0±1.0	Robie and Hemingway (1995)
	$Sb(OH)_3^{o}(aq)$	−644.4±1.1	Zotov et al. (2003)
	$Sb(OH)_2^{+}(aq)$	−415.2	Roper et al. (2012)

374
375
376

377

378   Table 3. Crystal data and structure refinement details for klebelsbergite.

Empirical formula	$Sb_4O_4(OH)_2SO_4$
Formula weight	681.08
Temperature	293(2) K
Wavelength	0.71073 Å
Crystal system	Orthorhombic
Space group	$Pca2_1$
Unit cell dimensions	$a = 5.7563(4)$ Å
	$b = 11.2538(7)$ Å
	$c = 14.8627(9)$ Å
Volume	962.81(11) $Å^3$
Z	4
Density (calculated)	4.699 g cm^{-3}
Absorption coefficient	11.358 mm^{-1}
$F(000)$	1208
Crystal size	0.15 x 0.10 x 0.08 mm
θ range for data collection	1.37 to 28.21°
Index ranges	$-5 \le h \le 7$, $-14 \le k \le 14$, $-19 \le l \le 19$
Reflections collected	9385
Independent reflections	2206 [R(int) = 0.0261]
Completeness to θ = 28.21°	95.2%
Refinement method	Full-matrix least-squares on F^2
Data/restraints/parameters	2206/3/144
Goodness-of-fit on F^2	1.117
Final R indices [$I > 2\sigma(I)$]	$R_1 = 0.0154$, $wR_2 = 0.0377$
R indices (all data)	$R_1 = 0.0154$, $wR_2 = 0.0377$
Absolute structure parameter	0.0(2)
Extinction coefficient	0.00151(8)
Largest diff. peak and hole	1.156 and -0.665 e $Å^{-3}$

379
380
381

382

383
384
385
386   Table 4. Atom coordinates and equivalent isotropic displacement parameters (Å^2 x 10^3) for
387   klebelsbergite. U_{eq} is defined as one third of the trace of the orthogonalized U^{ij} tensor.

	x/a	y/b	z/c	U_{eq}
Sb(1)	0.4792(1)	0.3598(1)	0.2754(1)	9(1)
Sb(2)	0.3927(1)	0.878(1)	0.1163(1)	7(1)
Sb(3)	0.1531(1)	0.4079(1)	0.4579(1)	7(1)
Sb(4)	0.478(1)	0.1410(1)	0.2926(1)	8(1)
S	0.8221(2)	0.2604(1)	0.0326(1)	8(1)
O(1)	0.6523(6)	0.2477(3)	-0.0419(3)	15(1)
O(2)	0.8534(7)	0.3868(3)	0.0536(2)	18(1)
O(3)	1.0424(6)	0.2032(3)	0.0093(3)	22(1)
O(4)	0.7252(6)	0.2020(3)	0.1148(2)	18(1)
O(5)	0.2818(6)	0.4624(3)	0.2025(3)	12(1)
O(6)	0.3127(6)	0.2056(3)	0.2091(3)	9(1)
O(7)	0.4243(6)	0.4908(3)	0.3905(2)	8(1)
O(8)	0.6145(6)	-0.0095(3)	0.1891(3)	9(1)
O(9)	0.2755(7)	0.0509(3)	0.3635(3)	14(1)
O(10)	0.2029(6)	0.3071(3)	0.3486(2)	10(1)
H(1)	0.381(8)	0.493(5)	0.166(3)	17[a]
H(2)	0.345(10)	0.094(4)	0.404(3)	20[a]

388   Note: [a]fixed in accord with the riding model.

389   Table 5. Anisotropic displacement parameters (Å^2) for klebelsbergite.

	U^{11}	U^{22}	U^{33}	U^{23}	U^{13}	U^{12}
Sb1	0.0067(2)	0.0109(1)	0.0092(2)	0.00078(12)	0.00111(12)	0.00070(10)
Sb2	0.0065(1)	0.0081(1)	0.0062(2)	-0.00010(12)	0.00009(12)	0.00058(9)
Sb3	0.0061(1)	0.0075(1)	0.0060(1)	0.00000(11)	0.00000(11)	0.00057(10)
Sb4	0.0070(2)	0.0099(1)	0.0082(2)	-0.00029(12)	0.00074(11)	0.00080(10)
S	0.0073(5)	0.0098(5)	0.0075(4)	0.0013(4)	0.0009(5)	0.0003(4)
O1	0.0147(2)	0.0178(2)	0.011(2)	-0.0016(14)	-0.0039(14)	0.0040(13)
O2	0.031(2)	0.0113(2)	0.013(2)	0.0021(14)	-0.0016(16)	0.0008(14)
O3	0.010(2)	0.032(2)	0.023(2)	-0.0135(16)	0.0004(15)	0.0072(15)
O4	0.022(2)	0.0224(2)	0.009(2)	0.0033(16)	-0.0001(16)	-0.0105(14)
O5	0.011(2)	0.0127(1)	0.014(2)	0.0028(14)	0.0002(14)	0.0007(13)
O6	0.010(2)	0.0070(1)	0.009(2)	-0.0022(13)	0.0017(13)	-0.0018(12)
O7	0.005(2)	0.0109(1)	0.008(2)	-0.0022(12)	0.0004(13)	-0.0020(12)
O8	0.005(2)	0.0106(2)	0.010(2)	0.0006(13)	0.0006(12)	0.0018(12)
O9	0.017(2)	0.0121(2)	0.014(2)	0.0010(15)	-0.0073(15)	0.0014(15)
O10	0.010(2)	0.0123(2)	0.008(2)	-0.0037(13)	0.0045(13)	-0.0036(12)

390 Table 6.   Bond lengths [Å] and angles [°] for klebelsbergite.

Sb(1)-O(5)	1.949(4)	Sb(2)-O(6)	1.968(3)
Sb(1)-O(10)	2.016(3)	Sb(2)-O(8)	2.000(3)
Sb(1)-O(6)	2.213(3)	Sb(2)-O(8)#1	2.123(3)
Sb(1)-O(7)	2.281(3)	Sb(2)-O(4)	2.306(3)
\<Sb-O\>	2.115	\<Sb-O\>	2.099
Sb(3)-O(10)	2.002(3)	Sb(4)-O(9)	1.963(4)
Sb(3)-O(7)#2	2.009(3)	Sb(4)-O(6)	2.097(3)
Sb(3)-O(7)	2.076(3)	Sb(4)-O(8)#1	2.170(4)
Sb(3)-O(1)#3	2.518(3)	Sb(4)-O(10)	2.232(3)
\<Sb-O\>	2.151	\<Sb-O\>	2.116
O(5)-Sb(1)-O(10)	90.8(2)	O(6)-Sb(2)-O(8)	98.0(2)
O(6)-Sb(1)-O(7)	141.3(1)	O(8)#1-Sb(2)-O(4)	149.6(1)
O(10)-Sb(3)-O(7)#2	90.7(1)	O(9)-Sb(4)-O(6)	90.6(2)
O(7)-Sb(3)-O(1)#3	147.9(1)	O(8)#1-Sb(4)-O(10)	139.9(1)
S-O(3)	1.464(4)	S-O(1)	1.483(4)
S-O(2)	1.467(3)	S-O(4)	1.495(4)
\<S-O\>	1.477		
O(3)-S-O(2)	111.8(2)	O(2)-S-O(1)	109.5(2)
O(3)-S-O(1)	110.6(2)	O(2)-S-O(4)	107.3(2)
O(3)-S-O(4)	108.8(2)	O(1)-S-O(4)	108.8(2)

D-H...A	d(D-H)	d(H...A)	d(D...A)	\<(DHA)
O(5)-H(1)...O(2)#2	0.86(2)	2.16(5)	2.819(5)	133(5)
O(5)-H(1)...O(5)#4	0.86(2)	2.42(5)	3.000(2)	125(5)
O(9)-H(2)...O(3)#5	0.87(2)	2.09(2)	2.955(5)	171(6)

391 Note: symmetry transformations used to generate equivalent atoms are #1: x-1/2,-y,z; #2: x-1/2, -
392 y+1,z; #3: -x+1/2,y,z+1/2; #4: x+1/2,-y+1,z; #5: -x+3/2,y,z+1/2.
393
394
395
396
397
398   Figure 1. Pourbaix diagram showing the stability field of klebelsbergite with respect to
399 some common secondary Sb minerals and stibnite; a, b and c refer to conditions where $a(SO_4^{2-})$
400 = 10^{-4}, 10^{-2} and 10^0, respectively.
401
402   Figure 2. The structure of klebelsbergite. Sb-centred polyhedra are coloured brown and
403 sulfate groups yellow. O and H atoms are indicated by red and white spheres, respectively, and
404 the unit cell is outlined.
405
406   Figure 3. The hydrogen bonding network in klebelsbergite viewed down a, slightly
407 rotated about c. Only sulfate and hydroxide ions are shown for clarity. S, O and H atoms are
408 brown, red and white, respectively. Full and hydrogen bonds are coloured grey and blue,
409 respectively, and the unit cell is outlined.

20